npj | heritage science

Article

https://doi.org/10.1038/s40494-025-01630-0

# Color characteristics of plum-green celadon glaze from the Longquan kiln in Southern Song (1127–1276 A.D.) and Yuan Dynasties (1271–1368 A.D.)

Check for updates

Zhen Sang[1], Le Li[1], Mingjun Wu[3], Zizhen Shen[3], Xuemei He[1], Pei Shi[4], Xiaojuan Yuan[2], Jing Gao[1] & Xiangyang Fu[1] ✉

Plum-green celadon is a quintessential example of Longquan kiln celadon varieties. This study explored the color characteristics of plum-green celadon by analyzing 19 glaze samples via various techniques, including colorimeter, XRF, XRD, Raman spectroscopy, and SEM/EDS. The results showed that the firing temperature of the Southern Song specimens was lower than that of the Yuan Dynasty specimens. Furthermore, phase-separated droplets within the glaze layers of specimens from both dynasties contributed to a Rayleigh scattering effect, which in turn subtly influenced the overall glaze color. The glaze coloration of Longquan plum-green celadon from the Southern Song and Yuan dynasties was the result of the interaction of chemical and physical factors.

The Longquan kiln, located in Longquan City, Zhejiang Province, China, includes prominent kiln sites such as Dayao, Xikou, and Jincun. Its origins trace back to the Wei and Jin Dynasties, with significant development occurring during the Northern Song Dynasty. The kiln reached its peak production during the Southern Song and Yuan Dynasties, followed by a gradual decline from the Ming to the Qing Dynasties. This remarkable longevity, spanning nearly 1,700 years, makes Longquan kiln the oldest continuously operating porcelain kiln in China[1]. Notably renowned for its celadon ware, glazes from Longquan kiln are characterized by their jade-like appearance and exquisite craftsmanship, establishing them as iconic examples of southern China's celadon production[2]. The plum-green celadon glaze color, particularly prominent during the Southern Song and Yuan Dynasties, is notable for its emerald green crystalline quality, jade-like gloss, and historical significance of its glaze color, signifying a key milestone in the evolution of Chinese celadon[3].

Current research on the Longquan kiln celadon has yielded significant findings. However, studies have predominantly focused on the chemical composition of celadon glazes and bodies, the production process, and related narrow facets, with limited emphasis on comprehensive investigations into the coloring mechanisms of Longquan celadon[4–6]. The mechanism behind the plum-green celadon glaze color remains largely elusive. Therefore, this research aims to uncover the scientific principles underlying the coloration of plum-green celadon glazes in Longquan, illuminating the unique beauty of the glaze coloration. This study conducts an in-depth exploration of chroma values, chemical composition, firing temperatures, iron ion chemical states, phases, and the microstructure of Longquan plum-green celadon glazes from the Southern Song and Yuan dynasties. And the effects of chemical and physical colors on glaze coloration were comprehensively examined. The color characteristics of Longquan plum-green celadon glaze are comprehensively and systematically analyzed, and the results provide a solid theoretical basis for both archaeological dating research and replication.

## Experimental procedure

### Experimental specimens

The Longquan celadon pieces used in this experiment were sourced from the Longquan Celadon Museum of Zhejiang Province, China. These artifacts consisted of plum-green celadon pieces from the Southern Song Dynasty, numbered S1–S10, and celadon pieces from the Yuan Dynasty, numbered Y1–Y9. Detailed digital photographs of the Longquan celadon pieces, along with descriptions of their body and glaze characteristics, are presented in Fig. 1 and Table 1, respectively.

### Experimental method

The colorimetric values of all specimens were measured using a colorimeter (X-rite, I4800, USA). An X-ray fluorescence spectrometer (EDXRF, XGT-

[1]School of Art and Design, Shaanxi University of Science & Technology, Xi'an, China. [2]School of Culture & Education, Shaanxi University of Science & Technology, Xi'an, China. [3]Longquan Celadon Museum, Longquan, China. [4]School of Material Sciences and Engineering, Shaanxi University of Science & Technology, Xi'an, China. ✉e-mail: xiangyangfu@foxmail.com

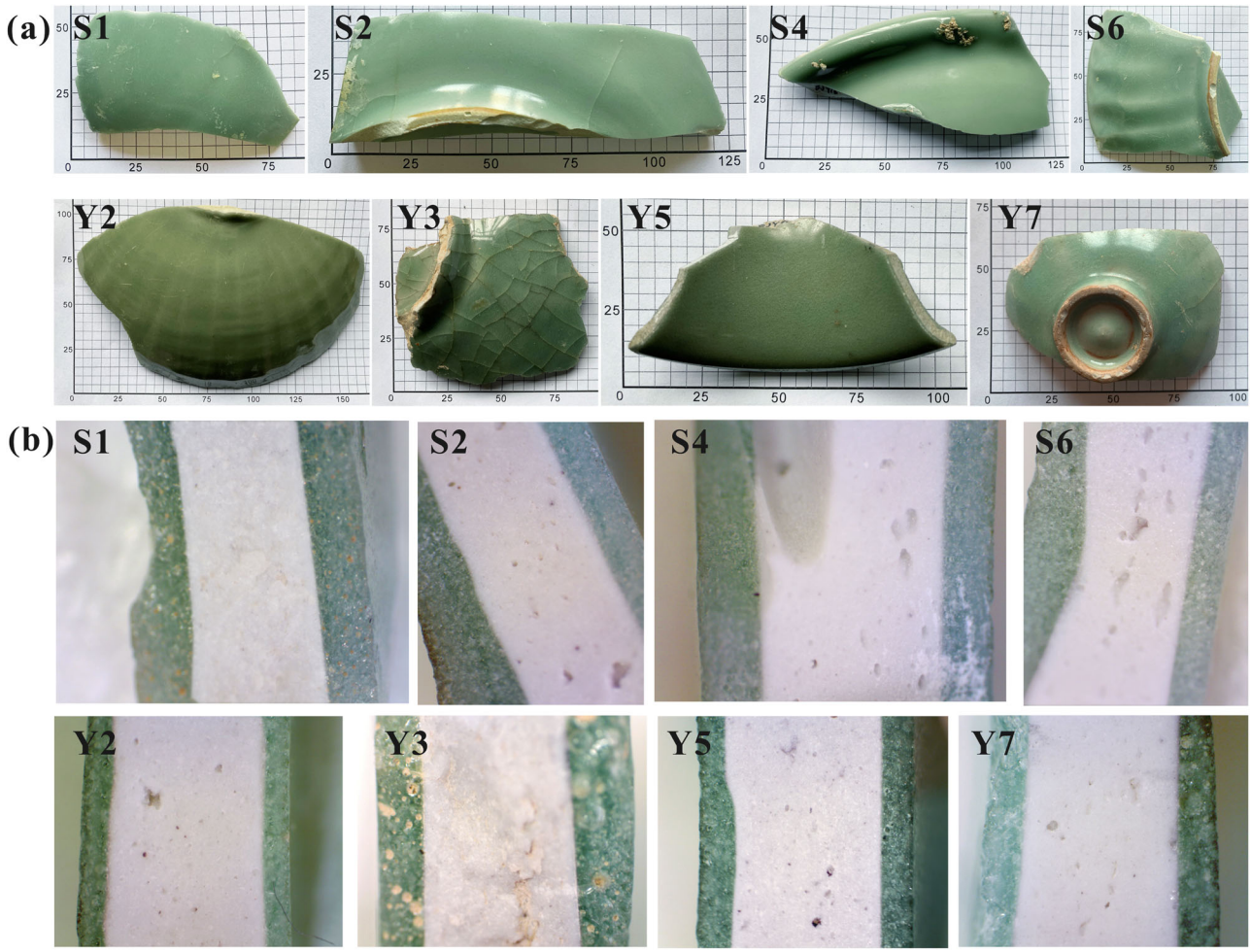


**Fig. 1 | Detailed digital photographs of the Longquan celadon pieces. a** Appearance of plum-green celadon shards from the Southern Song and Yuan Dynasties, Longquan kiln. **b** Cross-section of plum-green celadon shards from the Southern Song and Yuan Dynasties, Longquan kiln.

7200V, Japan) was used to analyze the chemical composition of all specimens. The physical phases of the specimens were determined via X-ray diffraction (XRD, Smart Lab 9 kW, Japan). The physical phases and molecular structures of the glassy phases in the specimens were studied using a micro confocal laser Raman spectrometer (Raman, Renishaw InVia, UK). Subsequently, the specimens were treated with 1 vol% hydrofluoric acid for 60 s, followed by ultrasonic cleaning in deionized water for 20 mins, and then dried. Finally, the microstructures and elemental compositions of the glazes in the specimens were examined via scanning electron microscopy (SEM, Zeiss Gemini 300, Germany) and energy-dispersive X-ray spectroscopy (EDS).

## Results and discussion

### Chromaticity value analysis

The chromaticity values (L*, a*, b*) were examined for the specimens dating from the Southern Song and Yuan dynasties. L* represents lightness and spans a range of 0–100, with the lightness of the object directly proportional to the L* value. The a* value denotes the shift in the red–green spectrum of the object, where positive values indicate a tendency toward red, and negative values indicate a preference for green. Similarly, the b* value represents the object's position in the color spectrum from yellow to blue, with positive values indicating a tendency toward yellow and negative values signifying a tendency toward blue.

Figure 2 presents the average L* value of the Longquan plum-green celadon glaze. The average brightness (L*) of the plum-green celadon glaze during the Southern Song and Yuan Dynasties was 53.62 and 50.38, respectively, with corresponding b* values of 6.74 and 7.09. The L* values from both dynasties were lower than those of Longquan light greenish-blue glaze, while their b* values were higher[7]. Conversely, Longquan plum-green celadon glaze appeared darker and yellower. Their color differences primarily originated from variations in chemical composition and firing temperature. The primary raw materials for Longquan celadon glaze include clay, porcelain stone, porcelain clay, limestone, and plant ash. In addition, plum-green celadon glaze incorporates purple clay, which enhances its $Fe_2O_3$ content and deepens its color tone[8,9]. Moreover, the firing temperature of plum-green celadon ranges from approximately 1260 to 1300°C, whereas light greenish-blue celadon is fired at a lower range of about 1200 to 1260°C[9]. The higher firing temperature of plum-green celadon results in an increased silicate glass content, a lower opacified texture, and a reduced L* value. The samples from the Southern Song Dynasty exhibited higher values than those from the Yuan Dynasty, and the average values of a* and b* were smaller than those of the Yuan Dynasty, indicating that the brightness of the glaze from the Southern Song Dynasty was greater than that of the Yuan Dynasty, with a glaze color inclination toward greenish tones in comparison to the Yuan Dynasty.

Ceramic glaze coloration can be categorized into two types: chemical and physical coloring. Chemical coloring arises from colorants, such as pigments, and the chemical composition of the glaze, including ionic valence. The principle behind chemical coloration is that when atoms or ions are excited, their electrons transition between energy levels. If the energy of these transitions matches the energy of photons in the visible spectrum, selective absorption of visible light occurs, resulting in various

colors. Physical coloring, also referred to as structural coloring, is produced by the selective reflection, transmission, scattering, or diffraction of light due to microstructures within the glaze, such as crystal phases and phase separation structures[10–12].

**Table 1 | Sample characteristics**

| Dynasty | Number | Body Thickness | Glaze Thickness |
|---|---|---|---|
| Southern Song | S1 | 2.8 | 1.1 |
| | S2 | 3.9 | 1.4 |
| | S3 | 2.9 | 1.0 |
| | S4 | 3.7 | 0.9 |
| | S5 | 3.8 | 0.8 |
| | S6 | 5.0 | 1.4 |
| | S7 | 4.5 | 1.2 |
| | S8 | 4.1 | 0.5 |
| | S9 | 2.6 | 1.5 |
| | S10 | 3.2 | 0.6 |
| | Average | 3.7 | 1.0 |
| Yuan | Y1 | 3.5 | 0.7 |
| | Y2 | 3.2 | 0.7 |
| | Y3 | 6.1 | 1.2 |
| | Y4 | 4.0 | 0.9 |
| | Y5 | 3.2 | 1.1 |
| | Y6 | 3.2 | 1.3 |
| | Y7 | 4.0 | 1.5 |
| | Y8 | 3.1 | 1.0 |
| | Y9 | 3.1 | 1.7 |
| | Average | 3.7 | 1.1 |

Note: units are in mm.

## Analysis of chemical coloration

**Analysis of glaze chemical composition.** Table 2 presents the chemical composition of Longquan plum-green celadon glaze from the Southern Song and Yuan dynasties. According to the glaze coefficient formula $b = RO/(RO + R_2O)$ (where RO represents alkaline earth metal oxides and $R_2O$ represents alkali metal oxides), values of $b \geq 0.76$ designate calcium glazes, $0.50 \leq b < 0.76$ designate calcium-alkali glaze, and $b < 0.50$ designate alkali-calcium glaze[13]. The average b values for the glazes of the Southern Song and Yuan dynasties were 0.52 and 0.50, respectively, indicating that both were calcium-alkali glazes. Overall, the chemical oxide compositions of the glazes from both dynasties were relatively similar, suggesting a stable glaze source from the Longquan area. The main ingredients of the glaze were grass ash, limestone, and porcelain stone, which was consistent with the findings of Duan et al.[14].

In a unified ceramic glaze system, a higher iron content typically results in a deeper glaze color[12,15]. The $Fe_2O_3$ contents in the glazes from the Southern Song and Yuan dynasties were low, with average values of 0.90% and 0.93%, respectively. While $Fe_2O_3$ reduced the brightness of the glaze color, the L* values of the Longquan celadons with lower $Fe_2O_3$ content did not exhibit high values owing to their thick glaze layers. The average glaze thickness of the Southern Song and Yuan Dynasty specimens was as high as 1.04 mm and 1.10 mm, respectively. Thicker glaze layers increase the light path within the glaze, enhancing absorption and resulting in a darker color[15]. Consequently, the slight differences in $Fe_2O_3$ content and glaze layer thickness contributed to the higher L* value observed in the Southern Song specimens compared with those from the Yuan Dynasty.

The average $K_2O$ contents in glazes from the Southern Song and Yuan dynasty specimens were 2.22% and 2.00%, respectively. However, the average $K_2O$ content in other Longquan celadons or representative celadons from northern Yaozhou kiln sky-green porcelain glazes was about twice that of the plum-green celadon glazes. Part of the Longquan plum-green celadon either did not utilize or used minimal grass ash as a raw material[16,17]. Furthermore, $K_2O$ contributed to the greenish-blue color of the glaze[18], making the Longquan plum-green celadon of the Southern Song Dynasty more greenish than that of the Yuan Dynasty. The low $K_2O$ and CaO contents in

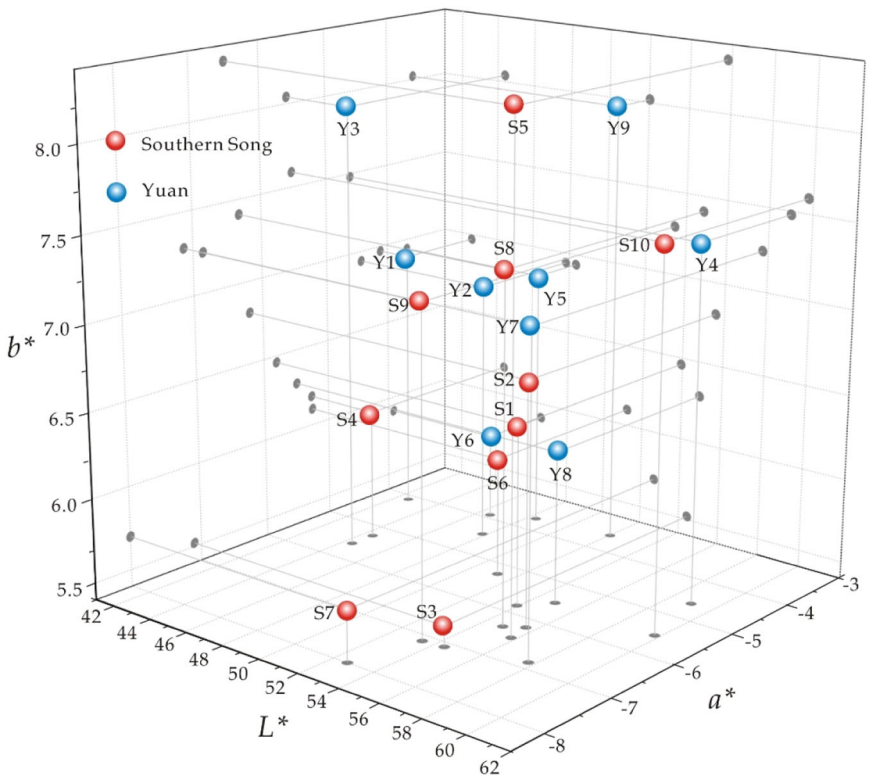


**Fig. 2 |** Sample of L*a*b* diagram.

**Table 2 | Chemical composition of Longquan celadon glazes from different dynasties (wt%)**

| Number | Dynasty | $Fe_2O_3$ | $Na_2O$ | MgO | $Al_2O_3$ | $SiO_2$ | $P_2O_5$ | $K_2O$ | CaO | $TiO_2$ | $MnO_2$ |
|---|---|---|---|---|---|---|---|---|---|---|---|
| S1 | | 0.95 | 3.11 | 0.89 | 13.67 | 75.95 | 0 | 2.33 | 2.89 | 0.07 | 0.12 |
| S2 | | 0.94 | 5.59 | 0.87 | 12.73 | 74.54 | 0 | 2.12 | 2.98 | 0.04 | 0.13 |
| S3 | | 0.95 | 2.98 | 1.16 | 13.65 | 75.17 | 0.04 | 2.09 | 3.71 | 0.06 | 0.18 |
| S4 | | 0.84 | 6.66 | 1.11 | 13.95 | 72.63 | 0.03 | 2.20 | 2.37 | 0.04 | 0.14 |
| S5 | Southern Song | 0.79 | 3.83 | 1.21 | 15.31 | 72.54 | 0.31 | 2.24 | 3.47 | 0.06 | 0.18 |
| S6 | | 0.82 | 5.05 | 0.86 | 13.36 | 74.8 | 0.01 | 2.20 | 2.71 | 0.04 | 0.11 |
| S7 | | 0.94 | 4.05 | 1.1 | 13.96 | 74.51 | 0.04 | 2.25 | 2.96 | 0.04 | 0.11 |
| S8 | | 0.89 | 4.09 | 1.24 | 13.17 | 74.80 | 0.12 | 2.37 | 2.99 | 0.06 | 0.26 |
| S9 | | 0.92 | 2.59 | 1.09 | 14.15 | 75.42 | 0.12 | 2.26 | 3.22 | 0.05 | 0.13 |
| S10 | | 0.97 | 2.61 | 1.13 | 13.45 | 75.75 | 0.12 | 2.14 | 3.62 | 0.05 | 0.12 |
| Average values for S1–S10 | | 0.90 | 4.06 | 1.07 | 13.74 | 74.61 | 0.08 | 2.22 | 3.09 | 0.05 | 0.15 |
| Y1 | | 0.99 | 4.67 | 1.60 | 13.96 | 71.25 | 0.18 | 2.08 | 4.91 | 0.05 | 0.29 |
| Y2 | | 0.92 | 4.05 | 1.54 | 12.49 | 75.95 | 0 | 2.24 | 2.41 | 0.06 | 0.31 |
| Y3 | | 0.86 | 7.04 | 0.84 | 12.84 | 72.96 | 0 | 2.04 | 3.28 | 0.04 | 0.08 |
| Y4 | | 1.10 | 2.64 | 1.64 | 14.57 | 74.29 | 0.12 | 2.03 | 3.34 | 0.05 | 0.19 |
| Y5 | Yuan | 1.22 | 4.35 | 1.31 | 17.4 | 69.92 | 0.13 | 2.21 | 3.15 | 0.10 | 0.16 |
| Y6 | | 0.64 | 5.37 | 1.25 | 11.44 | 76.68 | 0.04 | 1.96 | 2.42 | 0.05 | 0.13 |
| Y7 | | 0.72 | 5.83 | 1.18 | 13.17 | 73.14 | 0.18 | 2.02 | 3.5 | 0.06 | 0.15 |
| Y8 | | 0.86 | 1.77 | 1.26 | 14.04 | 76.47 | 0.08 | 1.76 | 3.53 | 0.05 | 0.15 |
| Y9 | | 1.05 | 5.21 | 1.79 | 14.02 | 71.14 | 0.40 | 1.70 | 4.44 | 0.05 | 0.16 |
| Average values for S1–S10 | | 0.93 | 4.55 | 1.38 | 13.77 | 73.53 | 0.13 | 2.00 | 3.44 | 0.06 | 0.18 |

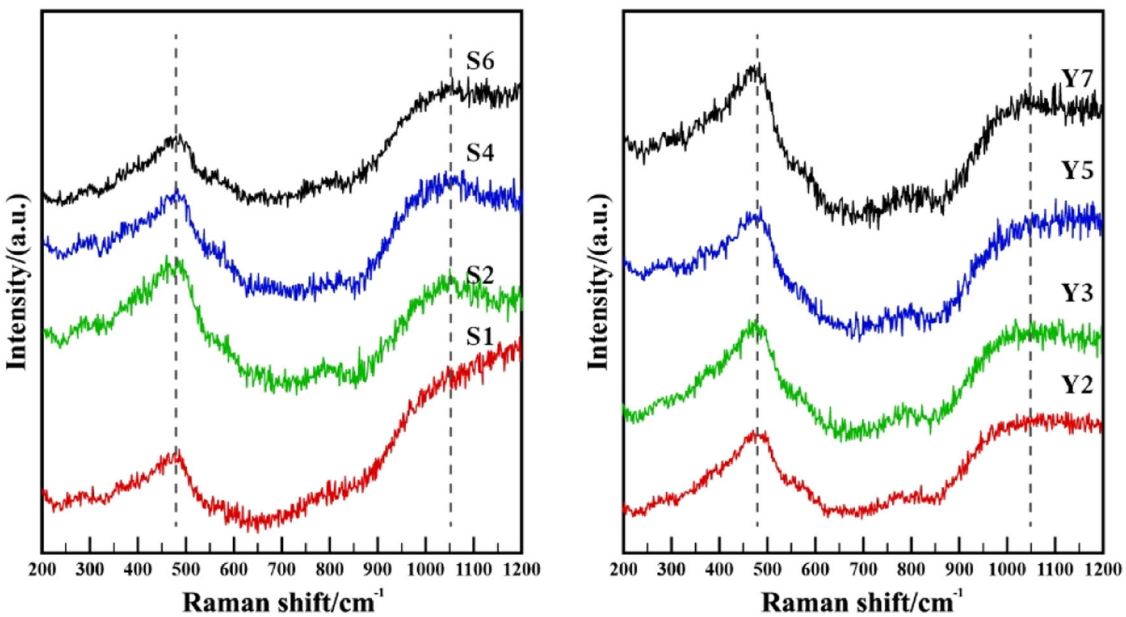


**Fig. 3** | Raman spectra on glaze surfaces of samples.

the specimens from both dynasties significantly increased the glaze's viscosity at high temperatures, resulting in thicker, less fluid glazes for Longquan plum-green celadon. All specimens exhibited low $P_2O_5$ content. $P_2O_5$ promoted phase separation during the glaze firing process, resulting in weaker coloration within the glaze phase structure. Additionally, both the firing temperature and the valence state of Fe ions had a significant impact on the glaze color. Representative glaze colors of both the Southern Song and Yuan Dynasties plum-green celadon specimens—S1, S2, S4, S6, Y2, Y3, Y5, and Y7 were selected for comparative Raman spectroscopy analysis to investigate the effect of firing temperature on the glaze color.

**Firing temperature analysis.** The Raman spectra and spectral fits of the specimens are shown in Figs. 3 and 4, respectively. All specimens exhibited two distinct Raman peaks at 486.8 $cm^{-1}$ and 1055.0 $cm^{-1}$, corresponding to the Si–O bending vibrational peak and the stretching vibrational peak within the [$SiO_4$] tetrahedron[19]. The area ratio of the bending to stretching vibrational peaks was related to the melting temperature. Therefore, the firing temperature of similar glazes was determined from the IP value of the Raman spectra, which was proportional to the firing temperature[20,21]. Gaussian fitting of the bending and stretching vibrational peaks of Si–O bonds in the specimen [$SiO_4$] tetrahedra was

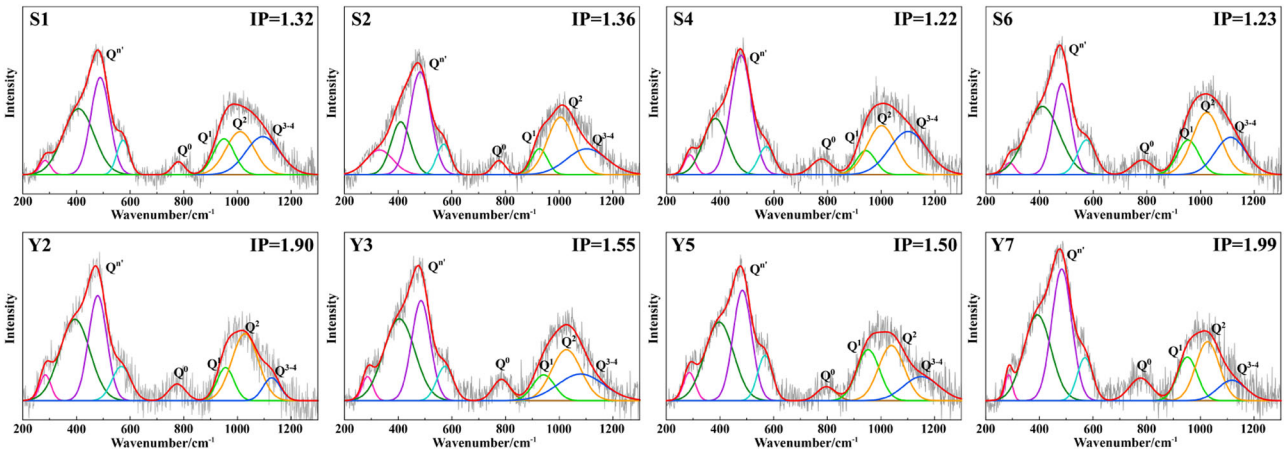


**Fig. 4** | Fitting Raman spectra of samples.

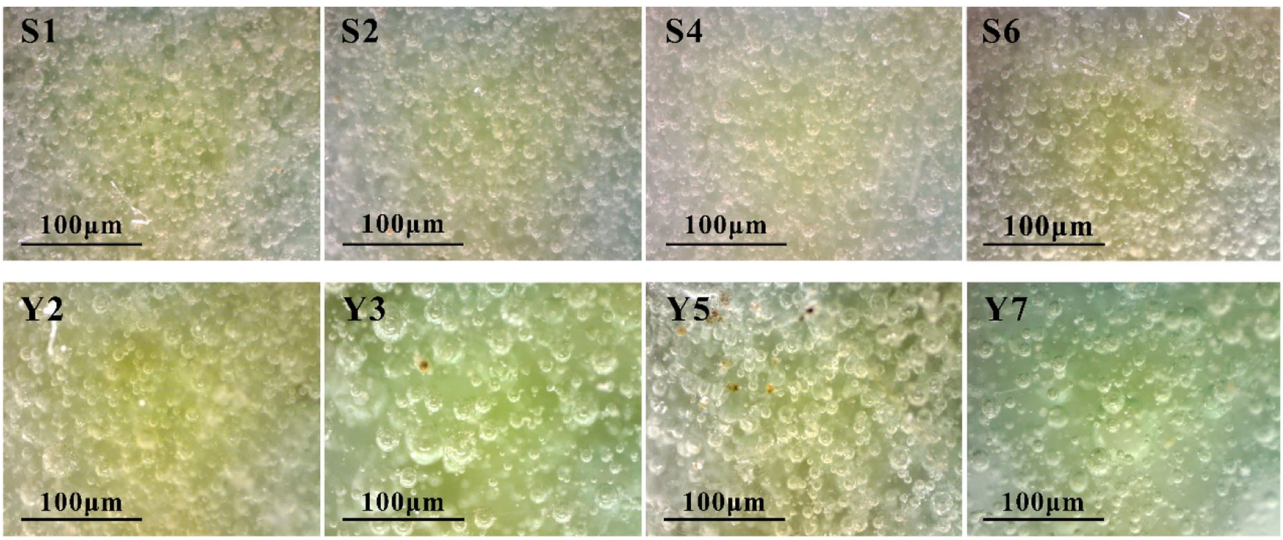


**Fig. 5** | Representative bubbles in the celadon porcelains of different dynasties.

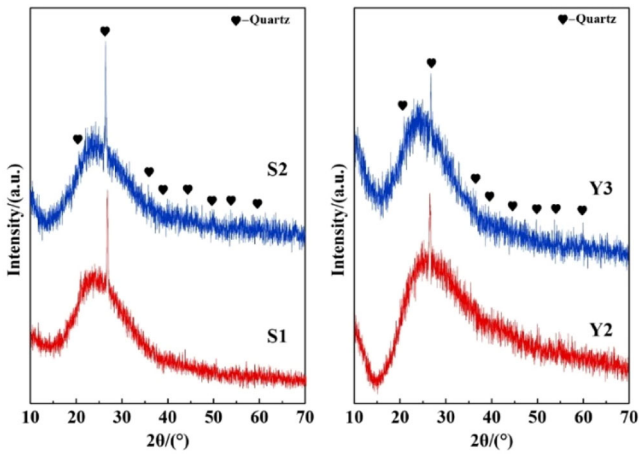


**Fig. 6** | XRD patterns on glaze surfaces of samples.

conducted to calculate the IP values of the specimens. The average IP values of specimens from the Southern Song and Yuan dynasties were 1.28 and 1.74, respectively. This result suggests that the firing temperature of Southern Song plum-green celadon was lower than that of the Yuan Dynasty. Generally, for similar glazes, firing temperature is directly proportional to the transparency, consistent with the glaze effect shown in Fig. 1.

### Physical coloration analysis

**Bubble analysis**. The formation of bubbles within the porcelain glaze was complex, resulting from gases that cannot be fully eliminated during firing, such as $H_2O$, $N_2$, and CO. Additional factors, such as reactions between the porcelain glaze and body, carbon formation, and processing conditions, also contributed to bubble formation[22]. Under certain conditions, the distribution, size, and density of bubbles in ancient porcelain can reveal aspects of the porcelain glaze formation mechanism. Figure 5 shows a digital photograph of bubbles in a representative Longquan plum-green celadon specimen from the Southern Song and Yuan Dynasties. Nano Measurer software was used to measure the bubble size of the specimen. The average bubble particle size for both dynasties was 6.87 μm and 8.92 μm, respectively, and the bubble density of the Southern Song specimen was greater than that of the Yuan Dynasty. During ceramic firing, the formation of bubble structures is closely related to the chemical composition and temperature of the glaze. An increase in $SiO_2$ content in porcelain glaze increases the viscosity of the glaze melt at high temperatures, further inhibiting bubble movement and coalescence. Consequently, bubbles become small and dense. The $SiO_2$ content in the Southern Song Dynasty samples (74.61%) was higher than that in the Yuan Dynasty samples (73.53%), resulting in smaller and denser bubbles

in the Southern Song Dynasty specimens[23]. Furthermore, increasing the firing temperature and extending the holding time of ceramics can enlarge bubble size and reduce density[24,25]. Given that the firing temperature in the Southern Song Dynasty was lower than that in the Yuan Dynasty, the observed bubble characteristics are consistent with these findings.

Bubbles in the glaze are generally spherical and possess a transparent or translucent texture. When light strikes the ceramic surface, the upper and lower surfaces of the bubbles reflect and refract light multiple times, resulting in a glazed surface with numerous densely packed bubbles reflecting more light toward the human eye. Consequently, ceramic glazes with dense bubbles exhibit higher whiteness, and increasing the L* value[26–29]. Therefore, the brightness and opalescence of the Southern Song specimens were higher than those of the Yuan Dynasty. Moreover, the transmittance of the glaze layer was inferior to that of the Yuan Dynasty. Additionally, when glazes use similar raw materials, a sparse distribution of larger bubbles generally corresponds to higher firing temperatures. Therefore, the firing temperature of the Southern Song specimens was lower than that of the Yuan Dynasty, aligning with the conclusions drawn from Raman IP value analysis. The representative glaze color specimens S1, S2, Y2, and Y3 were selected for an in-depth analysis of the crystals, microstructures, phases, and other physical coloration attributes of the plum-green glaze of the Southern Song and Yuan Dynasties.

**Crystal analysis of the glaze**. Figure 6 shows the XRD patterns of the glazes from Longquan plum-green celadon specimens S1, S2, Y2, and Y3 from the Southern Song and Yuan Dynasties. Notably, the patterns revealed very strong quartz crystal (quartz, PDF # 46-1045) diffraction peaks at 26.66° and 26.42°, with no significant diffraction peaks associated with other crystals. Thus, the crystals present in the glaze layer of

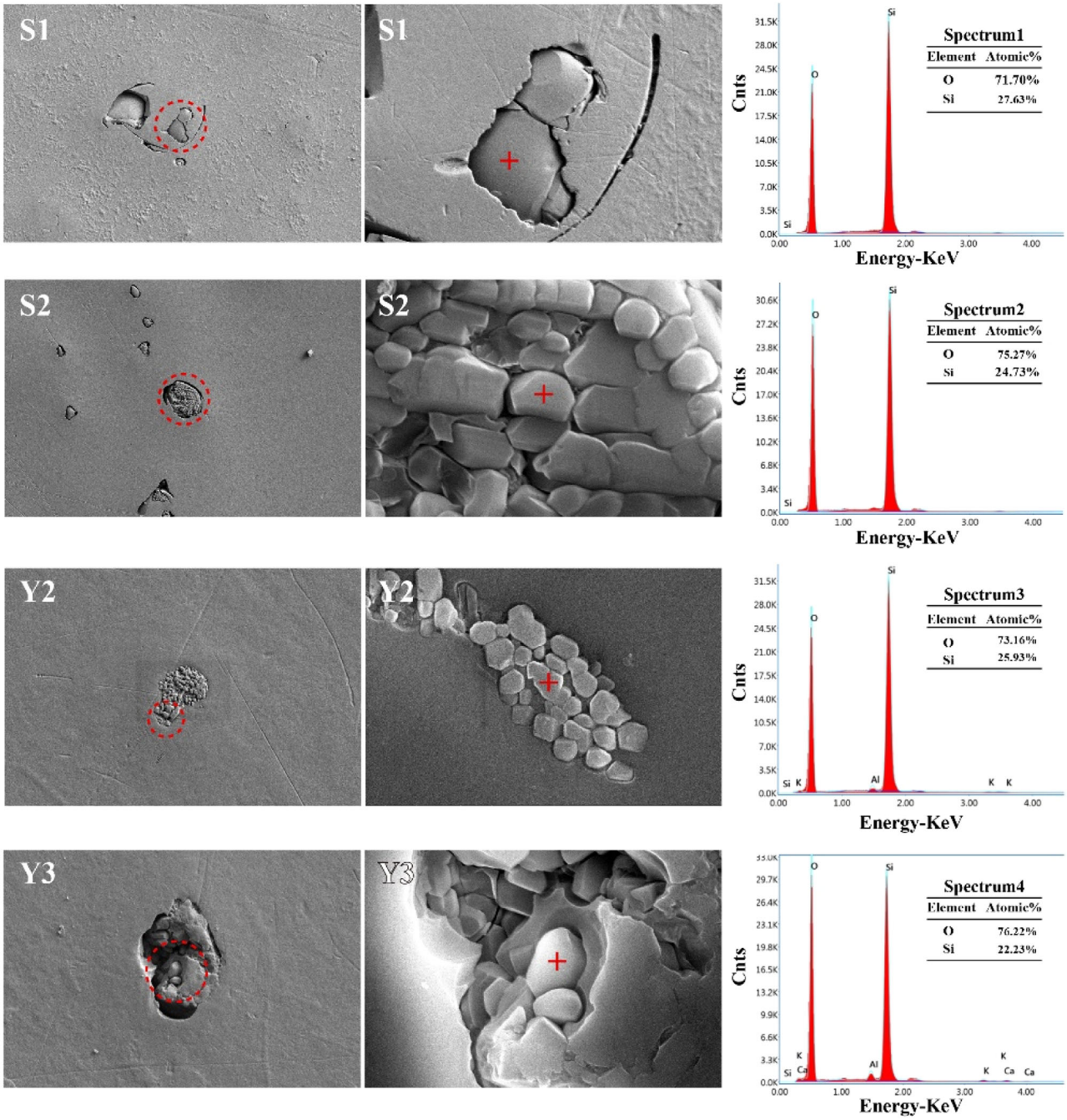


**Fig. 7** | SEM micrographs and EDS spectra of the etched glaze surface of S1, S2, Y2, and Y3.

Longquan plum-green celadon were basically quartz for both the Southern Song and Yuan Dynasties. Moreover, specimens S1, S2, Y2, and Y3 displayed strong amorphous diffraction peaks within the $2\theta \approx 15°$ –35 ° range. A large number of aluminum silicate glass phases occurred in the glaze layer. Under certain conditions, the glass phase content was proportional to the firing temperature of the porcelain glaze, so the firing temperature of the Yuan Dynasty specimens was higher than that of the Southern Song Dynasty, and leading to lower turbidity and reduced L* values in Yuan Dynasty glazes. Interestingly, no calcium feldspar crystals were detected within the glaze layers of the specimens. This absence was attributable to the higher firing temperatures, which likely caused the dissolution and disappearance of calcium feldspar formed during the firing process.

Figure 7 illustrates the SEM and EDS patterns of specimens S1, S2, Y2, and Y3 after hydrofluoric acid corrosion. Numerous square crystals were distributed within the glaze layer of the specimens. Chemical analysis via EDS revealed that Si and O were the dominant components in the composition, confirming that these crystals were predominantly quartz. Furthermore, owing to the similar refractive indices of quartz crystals (1.544) and the glass phase (1.500), their effect on the transmittance or opalescence of the glaze was relatively small[30]. However, the high crystal content in the glaze layer influences the opacity of the Longquan plum-green celadon specimens from both dynasties.

**Phase-separated structure analysis**. The SEM images (Figure 8) revealed the presence of densely distributed, spherical, phase-separated droplets within the glazes of specimens S1, S2, Y2, and Y3. The phase-separated structure within the porcelain glaze was a common occurrence, capable of producing structural colors under certain conditions. The phase-separated droplets were monodispersed, and their ability to create structural colors depended on their size and ordering. When the phase-separated droplets had a size of ~100 nm and exhibited noticeable short-range ordering without long-range ordering, they generated amorphous structural colors[31]. Additionally, when the size ranged from 5 nm to 100 nm, the phase-separated droplets were arranged without radial short-range ordering or angular uniformity (i.e., completely disordered), resulting in Rayleigh scattering. However, when the phase-separated droplets were spherical or nearly spherical, with an average size larger than 200 nm, they formed Mie scattering[32].

According to the SEM and 2D FFT diagrams in Figure 8, the phase-separated droplets in the glazes of S1, S2, Y2, and Y3 specimens belonged to a completely disordered structure, owing to the low content of $P_2O_5$ in the glaze. A certain amount of $P_2O_5$ was introduced into the silicate glass system, that is, in the form of cations with high charge and strong field strength, which could accelerate the formation and development of phase separation structures. The ionic potential of $P^{5+}$ is greater than that of $Si^{4+}$. The introduction of $P^{5+}$ would increase the free energy of the system at high temperatures, leading to instability. To reduce the free energy and form a stable glass, some bridging oxygen in the silicate network was replaced with $P^{5+}$, which broke the Si-O-Si bonds. $P^{5+}$ was then separated from the silicon-oxygen network along with $R^+$ or $R^{2+}$, resulting in a large number of phosphorus-rich silicon-oxygen network aggregates with small volumes. Owing to the significant differences in composition and density between these aggregates and the matrix silicate glass phase, forming a uniform silicon-phosphorus-oxygen glass with the matrix was challenging. However, these aggregates were uniformly dispersed in the matrix silicate glass as droplets, creating a phase-separated structure[33]. Therefore, the concentration of P ions influenced both the phase separation structure and the distribution of iron ions.

The relatively small size of the phase-separated droplets in the glazes of these specimens averaged around ~10 nm for those from the Southern Song Dynasty and ~5 nm for those from the Yuan Dynasty. The phase-separated droplets in samples S1 and S2 from the Southern Song Dynasty were larger than those in samples Y2 and Y3 from the Yuan Dynasty. This difference is attributable to the higher $Fe_2O_3$ content in samples S1 and S2 than that in Y2 and Y3. As the $Fe_2O_3$ content increased, the viscosity of the glaze melt decreased, resulting in larger phase-separated droplets[34]. These droplets were unable to form the amorphous structural colors and Mie scattering, but they met the criteria for Rayleigh scattering. The strongest Rayleigh scattering occurred when the size of the phase-separated droplet was 1/10 of the wavelength of blue light (i.e., 45–48 nm). Therefore, the glaze layers of Longquan plum-green celadon from both the Southern Song and Yuan Dynasties produced phase-separated structural color through Rayleigh scattering. However, the scattering effect was weak, resulting in only a slight impact on its color.

## Conclusion

(1) The source of the glaze in Longquan celadon remained stable in the Southern Song and Yuan Dynasties. According to the glaze

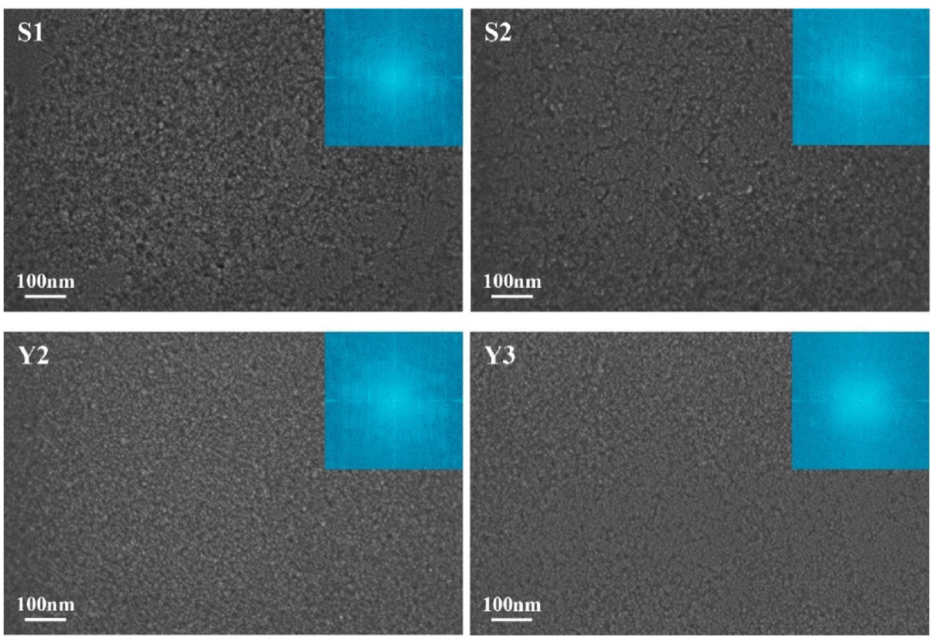


**Fig. 8** | 2D-FFT images of SEM results for specimens S1, S2, Y2, and Y3.

coefficient formula, the glaze of Longquan plum-green celadon specimens from both dynasties was classified as a calcium-alkali glaze. The low content of $K_2O$ and CaO contributed to the thickness of the Longquan celadon glaze, preventing it from flowing easily. The darker coloration of Longquan plum-green celadon was due to the increased thickness of the glaze. Additionally, the limited $P_2O_5$ content led to smaller phase-separated droplets in the glazes from the Southern Song and Yuan dynasties, reducing the influence of structural coloration on the glaze color.

(2) A comprehensive comparison of the glaze bubbles, crystal analysis, and Raman spectroscopy IP values from the two dynasties indicated that the firing temperature of Yuan Dynasty plum-green celadon specimens was higher than that of the Southern Song Dynasty.

(3) The Southern Song Longquan plum-green celadon specimens displayed smaller bubble sizes and higher densities than the Yuan Dynasty specimens, resulting in greater opacity. The specimens from both dynasties contained numerous quartz crystals within the glaze layer, which had a weak effect on glaze coloration. The phase-separated droplets within the glaze layer showed a completely disordered structure in both dynasties, generating weaker Rayleigh scattering, which had a limited impact on glaze coloration. Therefore, the "emerald green crystal, glossy as jade" appearance of Longquan plum-green celadon glaze from the Southern Song and Yuan dynasties resulted from an interplay between chemical and physical factors.

## Data availability

The datasets used during the current study are available from the corresponding author on reasonable request.

Received: 19 August 2024; Accepted: 21 November 2024;
Published online: 11 February 2025

## References

1. Zhu, B. Q. Celadon in Longquan Kiln. 1thed. Taipei: Artist Press; 1998.
2. The Chinese Ceramic Society. The history of Chinese pottery and porcelain. 1thed. Beijing : Cultural Relics Press; 1982.
3. Zhou, S. H. Further study on the celadon glaze in Longquan Kiln from the Song dynasty. *China Ceram.* **4**, 36–39 (1999).
4. Li, L. et al. Elemental Characterization by EDXRF of imperial Longquan Celadon Porcelain excavated from Fengdongyan Kiln, Dayao County. *Archaeometry* **57**, 966–976 (2015).
5. Feng, S. et al. Nondestructive analysis on ancient porcelain of Longquan Kiln in Zhejiang Province by WDXRF. *Chin. Phys. C.* **32**, 284–288 (2008).
6. Zhang, B., Zhang, M., Li, Y., Cheng, H. & Zheng, J. PIXE study on recovery of making-technology of Chinese Longquan celadon made in the Southern Song Dynasty (1127–1279 CE). *Ceram. Int* **45**, 3081–3087 (2019).
7. Sang, Z., Fu, X., Wu, M., Shen, Z. & Yuan, X. Study on the coloring mechanism of Longquan light greenish-blue celadon glaze from the Southern Song and Yuan Dynasties. *Ceram. Int.* **49**, 13249–13257 (2023).
8. Fang, J. Traceability, application and aesthetic features of dotting decoration technology of Longquan Celadon. *J. Shandong Univ. Art. Des.* **04**, 89–93 (2015).
9. Ye, H. et al. Study on Longquan celadon in Song Dynasty. *J. Ceram.* **02**, 64–78 (1999).
10. Sang, Z., Li, S., Yuan, X., Mu, Z. & Wei, X. Study on the separative-phase structural color of "Rose Purple Veins of Earthworm Crawling" of Jun Porcelain. *J. Shaanxi Univ. Sci. Technol.* **38**, 135–140 (2020).
11. Parker, A. Color in burgess shale animals and the effect of light on evolution in the Cambrian. *Proc. R. Soc. Lond. Ser. B* **265**, 967–972 (1998).
12. Wang, F. et al. Jun Ware glaze with opalescence, fambe, structural colors and chemical colors. *China Ceram.* **51**, 1–8+13 (2015).
13. Luo, H., Li, J. & Gao, L. Classification criteria of calcium glaze Types in Chinese ancient porcelain and its application in enamel research. *Bull. Chin. Ceram. Soc.* **2**, 50–53 (1995).
14. Duan, H. et al. Comparative study of black and gray body celadon shards excavated from Wayaoyang Kiln in Longquan, China. *Microchem J.* **126**, 274–279 (2016).
15. Lin, Y., Wang, F., Zhu, J. & Yang, H. Analysis of color change mechanism of Iron Ion in non-crystalline Solid. *China Ceram.* **48**, 13–15 (2012).
16. He, Z., Zhang, M. & Zhang, H. Data-driven research on chemical features of Jingdezhen and Longquan Celadon by energy dispersive X-ray fluorescence. *Ceram. Int* **42**, 5123–5129 (2016).
17. Sang, Z. et al. Analysis of the celadon characteristics of the Yaozhou kiln. *Ceram. Int* **45**, 22215–22225 (2019).
18. Shi, P. et al. Study on the coloring mechanism of the Ru celadon glaze in the Northern Song Dynasty. *Ceram. Int* **46**, 23662–23668 (2020).
19. Colombanp, P. & Paulsen, O. Non-destructive determination of the structure and composition of glazes by Raman Spectroscopy. *J. Am. Ceram. Soc.* **88**, 390–395 (2005).
20. Liem, N., Sagon, G., Quang, V. & Tan, H. Raman study of the microstructure, composition and processing of ancient Vietnamese (proto) porcelains and celadons (13–16th centuries). *J. Raman Spectrosc.* **31**, 933–942 (2000). Colomban.
21. El Amraoui, M. et al. Zelliges from Dar-El Beïda Palace in Meknes (Morocco): optical absorption and Raman spectrometry. *Spectrosc. Lett.* **40**, 777–783 (2007).
22. Zhang, J. H. Study on air bubbles in ancient ceramics. *Collect. World* **12**, 118–119 (2012).
23. Hu, Z. *Basic course of inorganic materials science*. (Chemical Industry Press, Beijing, 2004).
24. Sang, Z. et al. Study on the Colouring Mechanism of Moon-white Glaze of the Yaozhou Kiln in the Jin Dynasty. *China Ceram.* **57**, 75–81 (2021).
25. Zhao, Y. & Yin, H. Glass technology. Beijing: Chemical Industry Press; 2006.
26. Sang, Z. et al. Comparative Study on the Dating Characteristics of the Celadon of Yaozhou Kiln. *China Ceram.* **55**, 73–84 (2019).
27. Llusar, M. et al. Colour analysis of some cobalt-based blue pigments. *J. Eur. Ceram. Soc.* **21**, 1121–1130 (2001).
28. Zhu, T., Huang, H., Wang, H., Hu, L. & Yi, X. Comparison of celadon from the Yaozhou and Xicun kilns in the Northern Song Dynasty of China by X-ray fluorescence and microscopy. *J. Archaeol. Sci.* **38**, 3134–3140 (2011).
29. Shi, P. et al. Comparative study on celadon glazes of Five Dynasty Yaozhou kiln, Northern Song Dynasty Ru kiln and Southern Song Dynasty Guan kiln. *J. Chin. Silic. Soc.* **42**, 1935–1943 (2020).
30. Pagliari, L., Dapiaggi, M., Pavese, A. & Francescon, F. A kinetic study of the quartz-cristobalite phase transition. *J. Eur. Ceram. Soc.* **33**, 3403–3410 (2013).
31. Wang, Y. Light scattering theory and its application techniques. 1thed. Beijing : Science Press; 2013.
32. Colomban, P. Polymerization degree and Raman identification of aancient glasses uesed for jewelry, ceramic eenamels and mosaics. *J. Non-Cryst. Solids* **323**, 180–187 (2003).
33. Wang, F., Miao, J., Hou, J., Lin, Y. & Zhu, J. A study of iron oxide coloring function in blue glaze & green glaze jun porcelains. *Palace Mus. J.* **03**, 100–108 (2012).
34. Yang, Z. et al. Effect of iron oxide on the structure and coloring of jun porcelain opal blue glaze. *China Ceram.* **57**, 62–67 (2021).

## Acknowledgements

This work was supported by the National Natural Science Foundation of China (No. 52102026), the Key Science & Technology Program of Shaanxi Province of China (No. 2022GY-340), Research Project of Shaanxi Provincial Department of Education in China (No. 22JK0033) and the Graduate

Innovation Fund of Shaanxi University of Science and Technology (No. 2021BJ-14).

## Author contributions

Z.S.: Conceptualization,Writing-Original Draft, Supervision, Funding acquisition. L.L.: Methodology, Visualization, Investigation. M.W.: Resources. Z.S.: Resources. X.H.: Data Curation. X.F.: Writing—Review & Editing, Validation, Investigation. P.S.: Funding acquisition. X.Y.: Project administration. J.G.: Visualization, Funding acquisition.

## Competing interests

We declare that we have no known competing financial interests or personal relationships that could have appeared to influence the work reported in this paper.

## Additional information

**Correspondence** and requests for materials should be addressed to Xiangyang Fu.